University of Wollongong
Research Online

2016

Modelling of Dynamic Fracture Propagation in Coal Pillars using FLAC 2D

Gaetano Venticinque
University of Wollongong

Jan Nimcik
University of Wollongong

Modelling of Dynamic Fracture Propagation in Coal Pillars using FLAC 2D

Gaetano Venticinque and Jan Nemcik

ABSTRACT: For many years the empirical prediction of pillar stability has been the dominant method for pillar design. Now, with the advanced numerical modelling of dynamic fracture propagation, it is possible to study the correlation between the empirical pillar load estimates and the actual pillar fracture mechanics. An upgraded version to previously developed constitutive FISH subroutine in FLAC 2D driving the User-Defined-Model which simulates compressive failure behaviour of coal pillars through the development of dynamic fracture propagation. Special insight on peak strength and post failure behaviour is presented through analysis of fracture development as a function of the pillar width to height ratio. Results derived as part of this study show that the numerical fracture propagation in coal pillar produces similar results to the classical empirical estimations of pillar peak loads. The classical progressive shear failure in pillar ribs was observed in the models depicting the probable rib failure mechanisms. Such model is well suited towards providing better understanding of fracture behaviour in rock or coal mass to improve safety when mining within or around complex geological structures.

INTRODUCTION

A new method of modelling dynamic fracture propagation in rock has been used to simulate coal pillar failure modes. The new FISH code within the FLAC2D software was written to enable dynamic fracture to propagate through the rock, coal or similar materials. Several pillar geometries confined between competent roof and floor strata with various width to height (W/H) ratios of mined seam were modelled. The coal pillars were gradually loaded to failure and the progressive fracture propagation within the coal was simulated. For each pillar geometry, the modelled pillar strength was then compared against current popular empirical equation predictions.

THE FRACTURE MODEL

The dynamic fracture propagation model is a constitutive FISH based UDM in Itasca (2007) FLAC 2D geotechnical software; offering independent simulation of rock fracture initiation and propagation behaviour. This model has been previously verified for isotropic rocks where it was proved to offer realistic simulation of the brittle fracture and post failure response of rock in FLAC. In its current form, the model accommodates all three combinations of fractures: Mode I tensile, Mixed Mode I-II tensile shear and Mode III pure shear. This was verified through simulated application over the entire brittle-to-ductile transitional failure range of rock Venticinque (2013).

Simulation of Fracture Propagation in Coal Pillars

A new subroutine within the FLAC model was constructed to simulate coal pillar stress-strain response over the range of pre-and-post failure loading. This was performed for a number of pillar width to height (W/H) ratios listed in Table 1. Application of Venticinque's (2013) updated fracture model code was employed during each simulation to provide insight into key mechanisms of pillar failure achieved through the generation of real time dynamic fractures.

The typical geometry of modelled pillars is shown in Figure 1. Load was applied to the model through an application of steady strain loading at the grid surface boundary. The roof and floor were assumed competent whilst the properties of the coal seam were weaker in comparison. Due to the geological

School of Civil, Mining and Environmental Engineering, University of Wollongong, NSW, Australia. E-mail: jnemcik@uow.edu.au
M: 0408711280,

complexity of coal mass, the detailed structures such as the cleat and the bedding planes were not modelled. The properties of modelled rock layers are listed in Table 2.

Table 1: (W/H) Ratios of Simulated Coal Pillars

(W/H) Ratio	Width (m)	Height (m)
1:1	3.5	3.5
2:1	7.0	3.5
3:1	10.5	3.5
4:1	14.0	3.5
5:1	17.5	3.5
8:1	28.0	3.5

The typical geometry of modelled pillars is shown in Figure 1. Load was applied to the model through an application of steady strain loading at the grid surface boundary. The roof and floor were assumed competent whilst the properties of the coal seam were weaker in comparison. Due to the geological complexity of coal mass, the detailed structures such as the cleat and the bedding planes were not modelled. The properties of modelled rock layers are listed in Table 2.
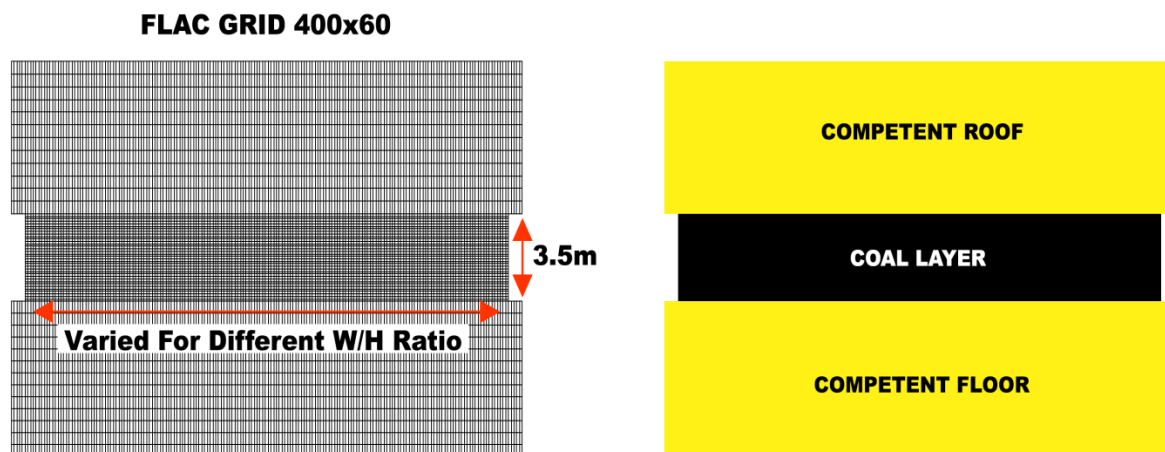

Figure 1: FLAC coal pillar model geometry

Table 2: Pillar model layer properties

Coal Layer Properties		Competent Roof and Floor Layer Properties	
Bulk Modulus (GPa)	3.3	Bulk Modulus (GPa)	20
Shear Modulus (GPa)	1.5	Shear Modulus (GPa)	12
Cohesion (MPa)	2	Density (kg/m^3)	2700
Tension (MPa)	1		
Internal Friction (°)	35		
Dilation (°)	6		
Density (kg/m^3)	1400		

Simulation Results

The average pillar load vs % of strain of all modelled pillars with various W/H ratios are plotted in Figure 2.

Modelled pillars are further investigated across Figures 4 to 9 which detail the progression of fracturing and key failure mechanisms over the entire (W/H) range.

At the early stages of pillar loading the fracture initiation and propagation begins at the pillar sides for all pillar sizes. Simulated fractures were predominately of a shear nature with dip angles approximately 60°

agreeing with the theoretical description of π/4 + Φ/2 for uniaxial loaded samples, (Jaeger and Cook 1971). Some minor tensile fractures also developed but did not influence the results greatly. As pillar loading increased, shear fractures were observed to work their way deeper into the pillars, Figure 3.
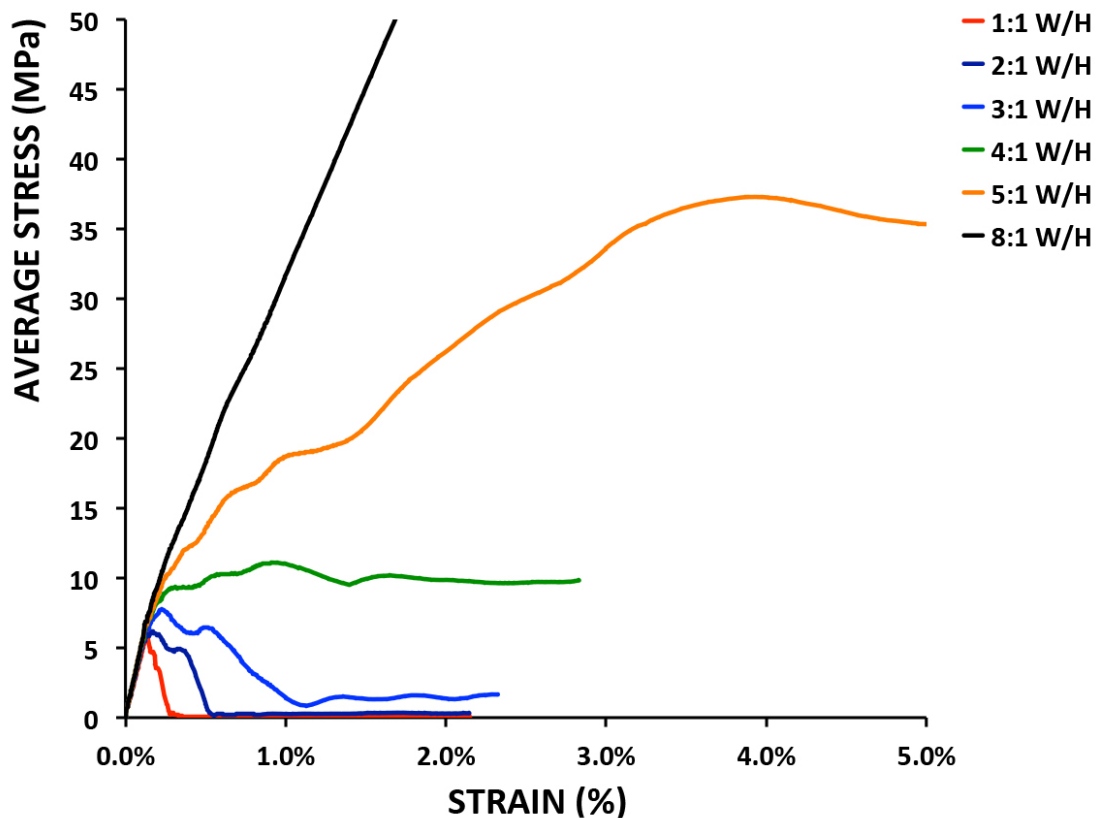

Figure 2: Average load vs strain for simulated coal pillar W/H ratios
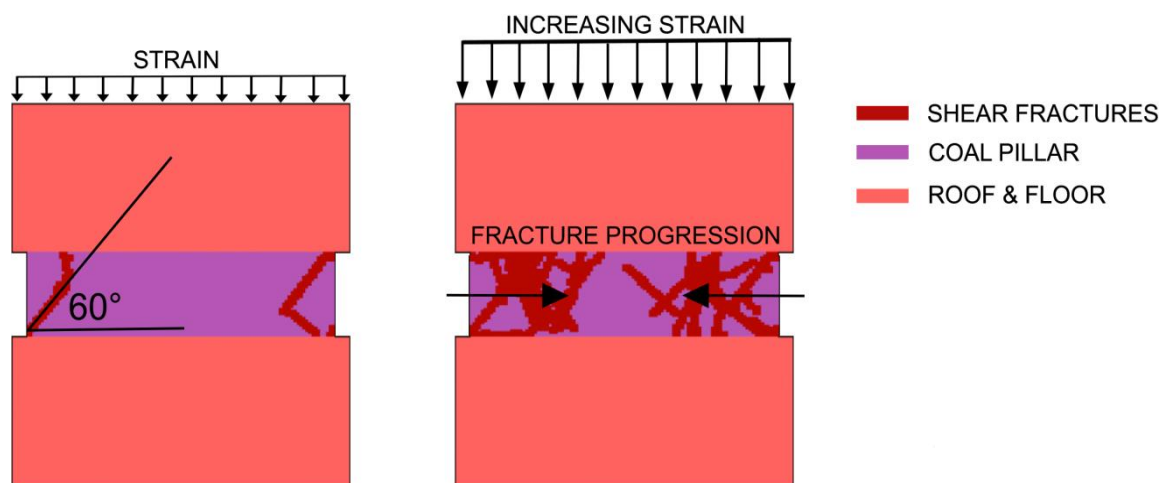

Figure 3: Progression of simulated fractures within modelled pillars

The narrow pillar (W/H = 1) failed at the maximum load of 6.3.MPa at the strain of 0.13%. The abrupt collapse of the pillar occurred early with no post failure strength and several shear fractures spanning between the roof and the floor as shown in Figure 4.
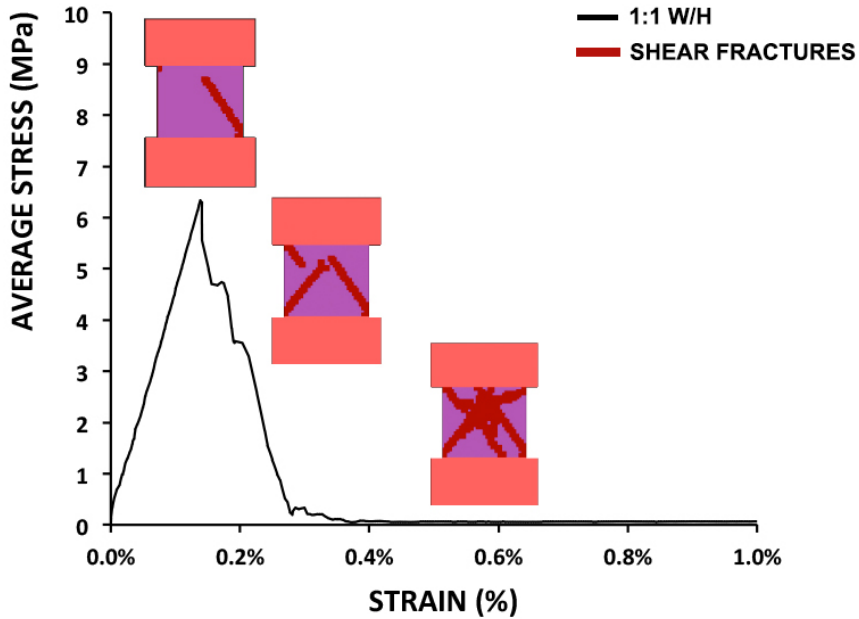
Figure 4: Average load vs strain and failure mode for pillar (W/H = 1)

The pillar of (W/H = 2) performed in a similar manner to the (W/H = 1) with slightly larger strain at failure as plotted previous in Figure 2. The coal pillar of (W/H = 3) developed early shear fractures at the pillar ribs with the fracture zone progressing deeper into the pillar as the vertical load increased. The modelled peak pillar load reached 7.8 MPa while the pillar post failure strength gradually reduced to low values indicating pillar inability to support additional load at greater strain. The load history versus the pillar strain and the fracture locations are shown in Figure 5.
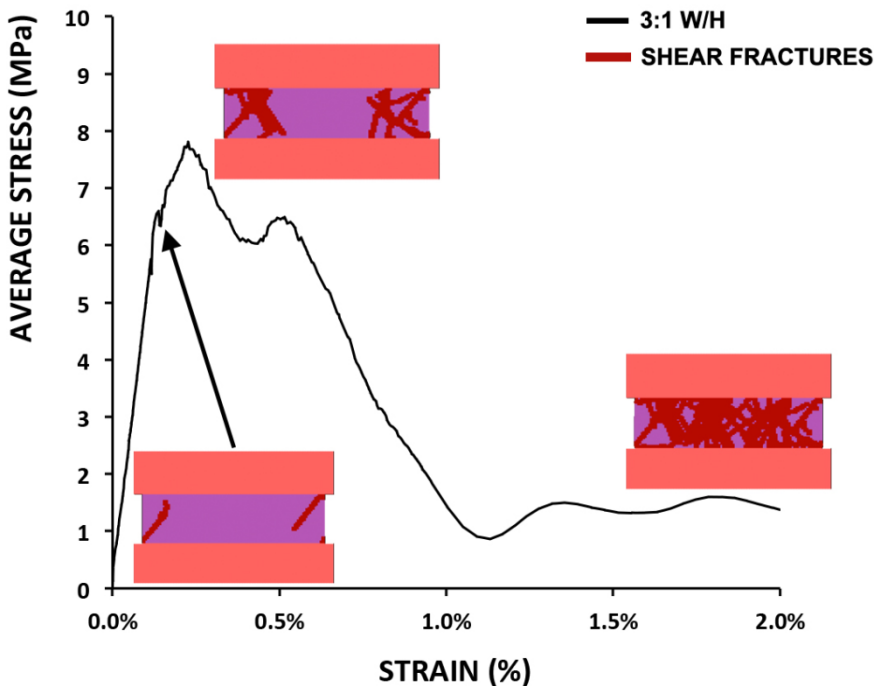

Figure 5: Average load vs strain and failure mode for pillar (W/H = 3)

It can be seen in Figure 5 that the post failure capacity of the pillar (W/H = 3) can be either zero or close to zero. It is noted that the waviness of the stress strain curve is related to subsequent individual fracture propagation.

For the (W/H = 4) the increasing vertical load caused the progressive rib shear failure to continue deeper into the pillar sides reaching the pillar centre at the strain of 0.85%. The maximum pillar load prior to total coal failure reached 11.1 MPa followed by a minor reduction in post failure pillar bearing capacity between 9.5 to 10 MPa, shown in Figure 6.
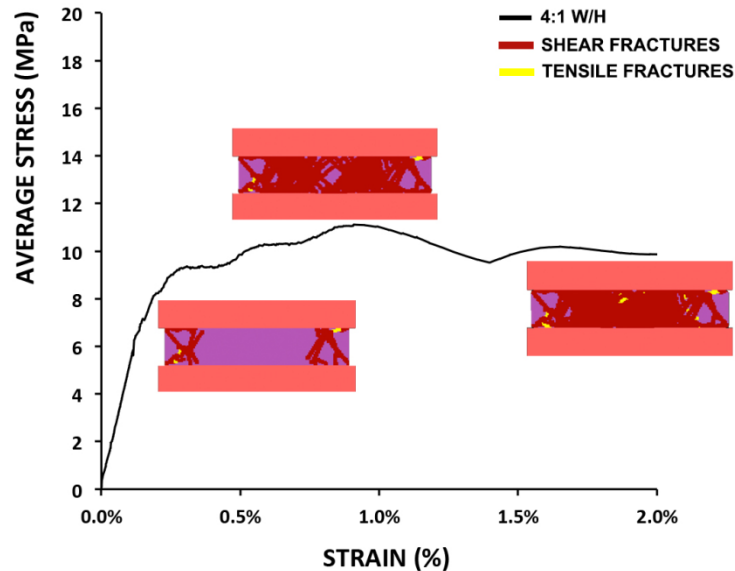

Figure 6: Average load vs strain and failure mode for pillar (W/H = 4)

The coal pillar with (W/H = 5) geometry followed the trend of the progressive pillar shear failure shown in Figure 6 with the maximum pillar capacity of 37.3 MPa. The pillar post failure strength stabilised at approximately 34 MPa indicating that even under higher strain the pillar will always carry some residual load bearing capacity. The wider coal pillar model of (W/H = 8) followed a similar progressive failure trend, Figure 8; however, the ability to accept the increasing load continued with the increase of strain. This behaviour conforms with anticipated mechanics of pillar coal systems described by Gale (1999).
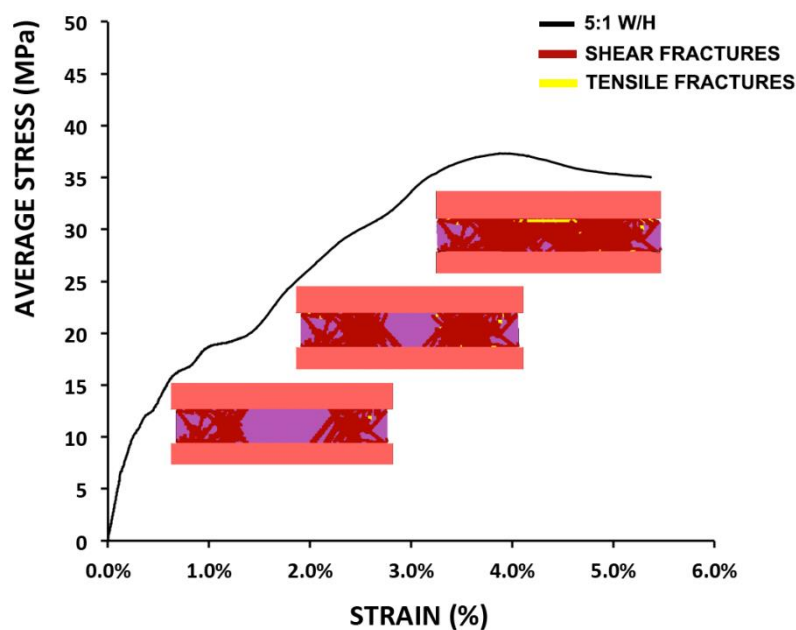

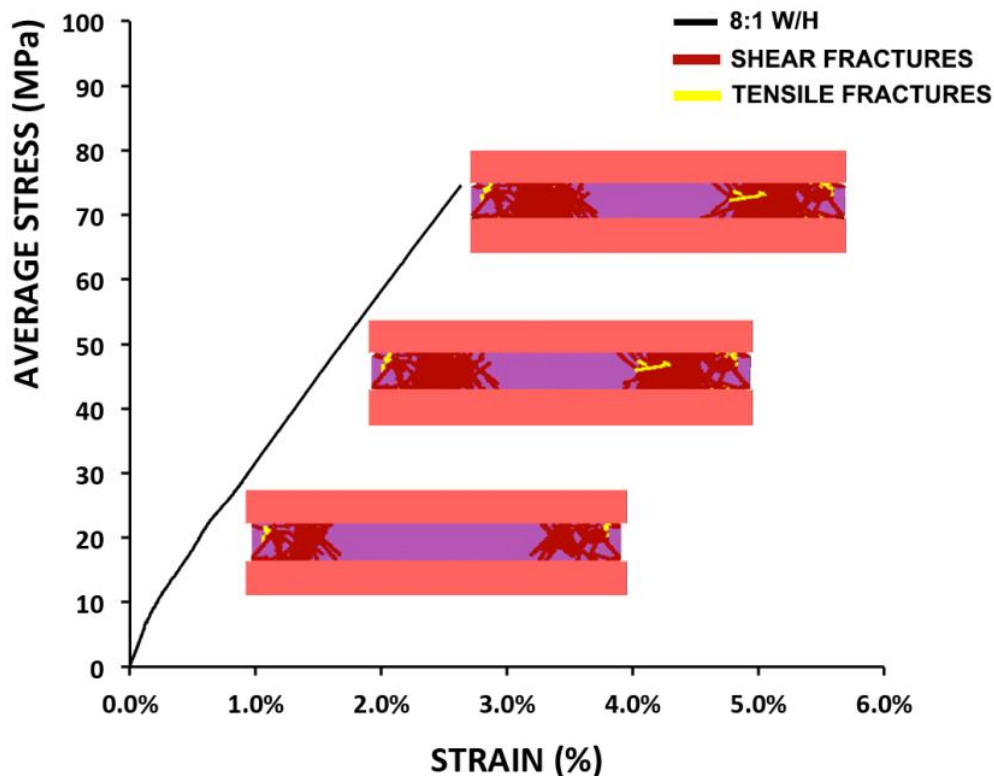**Figure 7: Average load vs strain and failure mode for pillar (W/H = 5)**

Figure 8: Average load vs strain and failure mode for pillar (W/H = 8)

Through assessing the progressive failure within the coal pillars at various (W/H) ratios, several important observations became apparent and are summarised below:

- (W/H = 1), Peak load of 6.3 MPa at strain of 0.13%.
- Note: The dynamic fracture propagation in the small pillar can be abrupt with no post failure strength. The peak load that the pillar can sustain is close to the *in situ* coal strength.
- (W/H = 3), Peak Load of 7.8 MPa at strain of 0.23%.
- Note: The pillar exhibits fast but more gradual fracture propagation towards the centre. Very small post failure strength was observed.
- (W/H = 4), Peak load of 11 1 MPa at strain of 0.95%.
- Note: The pillar exhibits gradual fracture propagation towards the centre. The stress-strain curve resembles an elastic-plastic behaviour.
- (W/H = 5), Peak load of 37.3 MPa at strain of 3.93%.
- Note: The pillar gradually yields towards the centre. The stress-strain shows strain softening behaviour with the maximum load peaking at a relatively high strain.
- (W/H = 8), No peak load, load continues to increase with strain.
- Note: Gradual yielding from the pillar edges eventually stops at 8 m from the pillar ribs.

COMPARISON OF MODELLED PILLAR STRENGTH WITH EMPIRICAL FORMULAS

The ultimate compressive load that the modelled coal pillars were able to carry were compared against empirically derived methods. In this analysis three well known empirical methods by Salamon-Munro (1967), Holland and Gaddy (1964) and Bieniawski (1992) were selected for comparison against simulated pillar strengths. The respective equations along with calculated values are given in Table 3 and 4 with results plotted in Figure 9.

Table 3: Empirical Coal Pillar Strength Formulas

Empirical Method	Formula	Key
Salamon and Munroe (1967)	$\sigma_p = 7.2 \times \dfrac{W^{0.46}}{H^{0.66}}$	W = Pillar Width H = Pillar Height
Holland and Gaddy (1964)	$\sigma_p = \dfrac{k\sqrt{W}}{H}$	k = Constant Relating to UCS σ_p = Peak Pillar Strength
Bieniawski (1992)	$\sigma_p = \sigma_1(0.64 + 0.36 \times \dfrac{W}{H})$	σ_1 = UCS

Table 4: Calculated strengths for coal pillar W/H ratios simulated

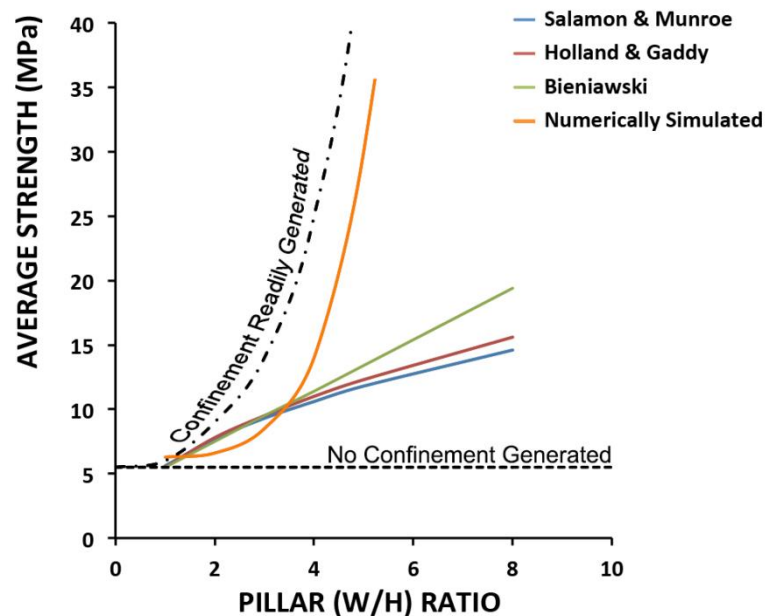| (W/H) Ratio	Peak Pillar Average Strengths (MPa)			
	Salamon and Munroe	Holland and Gaddy	Bieniawski	Numerically Simulated
1:1	5.6	5.5	5.5	6.3
2:1	7.7	7.8	7.5	6.6
3:1	9.3	9.5	9.5	7.8
4:1	10.6	11.0	11.4	11.1
5:1	11.8	12.3	13.4	37.3
8:1	14.6	15.6	19.4	Peak Load Undefined

Figure 9 – Comparing peak pillar strength vs W/H ratios for simulated coal pillars

Discrepancies between empirical methods and deviation of calculated strengths particularly for (W/H > 4) reflects a general limitation of empirical formula to be over conservative at (W/H > 5) as shown in Figure 9. Empirical approaches are henceforth recognised to be applicable only for conditions similar to those under which they were developed (Jaiswal 2009). Given the conditions simulated the results indicate that the correlations between the empirical pillar strength predictions and the modelled pillar

peak loads for various pillar geometries (W/H) ratios is good. Noted ability of numerical methods is highlighted where they are better capable of performing analysis of pillars with (W/H > 4) without being overconservative.

CONCLUSION

Overall, good comparison between the empirical data and the numerical model indicate that that the fracture mechanics within the model are realistic and can be used to study the sudden or progressive rib failure mechanisms that exist underground. In the empirical prediction of pillar failure the coal has to be the weakest component of the system. This does not apply to the numerical models where fractures can propagate in any location whether in the roof, coal seam or the floor strata. This makes the model more desirable to study the influence of the roof, coal or floor strata failure on the maximum pillar load. In many cases the weak contacts between the coal and the rock strata can significantly reduce the pillar stability Gale (1999). Likewise, excessive roof and/or floor failure in adjacent mine roadways can also influence the pillar strength by reducing the ability of the stiffer rock strata to provide lateral confinement to the coal seam. This numerical model has no problem in modelling such cases. Further research is planned to study how the coal cleat and laminations affect the fracture propagation in the coal mass. This study would enable more accurate predictions of the pillar strength. Through continued validation and additional application towards other complex problems Venticinque's (2013) model is envisaged to offer better, safer, more stable and efficient results to the mining and wider geotechnical industries.

REFERENCES

Bieniawski, Z T, 1992, A method revisited: coal pillar strength formula based on field investigations, proceedings, workshop on coal pillar mechanics and design, Bu mines, pp 158-165.

Gale, W J, 1999. Experience of field measurement and computer simulation methods for pillar design, *Proceedings Second International Workshop on Coal Pillar Mechanics and Design*, NIOSH IC 9448.

Holland, C T, 1964. The Strength of Coal Pillars, *Proceedings 6th US Symposium on Rock Mechanics*, University of Missouri, Rolla, pp 450–466.

Itasca Consulting Group, I, 2007. FLAC - fast lagrangian analysis of continua, *Version 7.0, User Manual*. Minneapolis.

Jaiswal, A and Shrivastva, B K, 2009. Numerical simulation of coal pillar strength, *International Journal of Rock Mechanics and Mining Sciences*, Volume 46, 779-788.

Jaeger, J C and Cook, N G W, 1971. Fundamentals of rock mechanics, *Chapman and Hall*, London.

Salamon, M D G, 1967. A method of designing board and pillar workings, *J. S. Afr. Inst. Min. Metall.,* 68: 68–78.

Venticinque, G A, 2013. Advanced Numerical Modelling of Fracture Propagation in Rock, *Honours Thesis, Department of Engineering, School of Mining Engineering, University of Wollongong*.

Venticinque, G A, Nemcik, J A and Ren, T, 2013. New fracture model for the prediction of longwall caving characteristics, *6th International Symposium on Green Mining* (ISGM), 2013, University of Wollongong.